Early Expression of the Gene for Interphotoreceptor Retinol-binding Protein during Photoreceptor Differentiation Suggests a Critical Role for The Interphotoreceptor Matrix in Retinal Development

Federico Gonzalez-Fernandez and Jim I. Healy

Department of Pathology, Division of Neuropathology, University of Virginia Medical Center, Charlottesville, Virginia 22908

Abstract. Interphotoreceptor retinol-binding protein (IRBP), the major protein component of the subretinal space, is in a strategic position to mediate cellular interactions between the retinal pigmented epithelium (RPE) and the neural retina. While IRBP appears to be involved in vitamin A transport during the visual cycle in the adult, the role of this protein during eye development has not been determined. As a first step to understanding the role of IRBP during retinal development, we have studied the expression of the mRNA for this glycolipoprotein during photoreceptor differentiation in the rat. A rat neural retina cDNA library was prepared from which an IRBP clone was isolated. The clone contains an open reading frame followed by a 3' noncoding sequence ending in 10 adenosine residues. The coding region has an identity of 83.9 and 82.5% with the nucelotide sequence of human and bovine IRBP, respectively. Rats (Sprague-Dawley, Wistar, and Royal College of Surgeon pink-eyed controls) have a 6.4 and a 5.2-kb mRNA for IRBP which are present in a 1:4 ratio and thus are the only vertebrate known to definitely have more than one major form of the IRBP message. Genomic Southern blots are consistent with the hypothesis that there is only one allele of the IRBP gene, suggesting that the two forms are produced by alternative processing of the mRNA. To generate an antisense RNA probe for use in molecular titration assays and Northern blots, an Eco RI–Bam HI fragment from the coding region was subcloned in between flanking Sp6 and T7 promoters. Total RNA was prepared from undissected rat globes from postnatal days p0–p22. The expression of the mRNA for IRBP was studied by Northern blots and the level of the transcripts determined by solution hybridization assays. Approximately 10^5 IRBP mRNA transcripts/μg total eye RNA are present at birth. This increases to a final level of 3.1×10^6 transcripts/μg total RNA by p9. The one-half maximal level of the mRNA occurs at p4.2 which is 2 wk before the one-half maximal level of IRBP is reached in the subretinal space (Gonzalez-Fernandez, F., R. A. Landers, P. A. Glazebrook, S.-L. Fong, G. I. Liou, D. M. K. Lam, and C. D. B. Bridges. 1984. *J. Cell Biol.* 99:2092–2098). The expression of the mRNA for IRBP reflects the developmental emergence of the interphotoreceptor matrix as an important structure within the retina. The absolute level of IRBP is related to the volume of the subretinal space, which expands during development due to the elongation of the outer segments. The unexpected early expression of the mRNA for IRBP during retinal development suggests that the interphotoreceptor matrix is important not only to the adult during the visual cycle, but also plays a critical role during retinal development, perhaps facilitating the diffusion of hydrophobic nutrients and morphogens such as vitamin A from the RPE/choroid complex to the growing and differentiating neural retina.

T HE interphotoreceptor matrix fills the subretinal space, separating the retinal pigmented epithelium (RPE)[1] and choroid capillaris, the blood supply of the photoreceptors, from the neural retina. Because of its unique location, the interphotoreceptor matrix may be involved in a variety of functions including facilitated diffusion of nutrients (39, 61), retinal adhesion (60), and embryonic induction (58). Nutrients and morphogens derived from the choroid or RPE must cross this extracellular matrix in order to reach the neural retina. The major protein component of the interphotoreceptor matrix is a 145-kD glycolipoprotein termed interphotoreceptor (or interstitial) retinol-binding protein (IRBP) (3, 13, 15, 27, 42, 49, 51, 54). IRBP is synthesized by the

---

1. *Abbreviations used in this paper:* IRBP, interphotoreceptor retinol-binding protein; RPE, retinal pigmented epithelium.

photoreceptor cells and secreted into the subretinal space (23, 24, 26, 32, 38, 50, 52, 56). The protein carries endogenous vitamin A in a light-dependent manner and is believed to facilitate the diffusion of vitamin A through the subretinal space in the adult retina during the visual cycle (1, 12, 37, 38, 41, 42, 47, 51). This intercellular traffic is essential because the isomerase needed for visual pigment regeneration is located in the RPE (5, 11). The precise role of IRBP in the extracellular transport of vitamin A between the pigmented epithelium and neural retina is not clear. One study has suggested that the protein functions to provide an extracellular buffer to vitamin A rather than a transport vehicle (31). In any event, light-evoked changes in the distribution of IRBP in the subretinal space may provide the motive force for the transfer of retinoids between the photoreceptors and pigmented epithelium (57).

The presence of IRBP during early retinal development before significant outer segment formation suggests that this protein may have a yet unrecognized role during retinal development (9, 14, 19, 20, 36). To understand the role of IRBP during retinal development, we have studied the expression of the mRNA for IRBP during photoreceptor differentiation in the rat. Rodents are well suited to the study of retinal development because most rod cells become postmitotic during the early postnatal period allowing their whole sequence of development to be studied conveniently (see Fig. 1). As with other vertebrates, the rat retina begins as an invagination of the optic cup which brings the RPE and primitive neuroblastic epithelium together. The apposition of these two layers is necessary in order for neuronal differentiation to occur (58). The cavity optic vesicle is obliterated when the RPE and neuroblastic epithelium become linked by junctional complexes (22). Shortly before birth in the rat, the two layers separate as interphotoreceptor matrix begins to accumulate between them. By postnatal day 5 (p5) the interphotoreceptor matrix has greatly expanded as the inner segments protrude into the subretinal space (21, 59). By p10, primitive outer segments can be seen by EM on the ends of most of the inner segments. During the following week, the bulk of rhodopsin synthesis occurs until the outer segments achieve their adult length (9, 14, 26, 28, 55).

In the present work, a rat IRBP cDNA was cloned and the postnatal levels of the mRNA for IRBP studied, by Northern blot analysis and solution hybridization assays. The findings suggest that IRBP may have a critical role during retinal development in addition to its role in the extracellular transport of vitamin A in the adult retina. A preliminary report of this work has been published as an abstract (Gonzalez-Fernandez, F., and C. D. B. Bridges. 1989. *J. Neuropathol. & Exp. Neurol.* 48:361.).

Materials and Methods

Library Construction and Screening

336 eyes were enucleated from light-adapted adult male and female Sprague-Dawley rats. After the anterior chamber was excised and the vitreous removed, the neural retina was detached from the RPE under PBS. The neural retinas were immediately frozen on dry ice and stored in liquid nitrogen. Total RNA was extracted by homogenization in quanidinium hydrochloride followed by ultracentrifugation on a cesium chloride gradient (46). Poly(A$^+$) RNA was isolated by affinity chromatography on oligo(DT)-cellulose (type 3, Collaborative Research, Lexington, MA). First strand

cDNA was synthesized using reverse transcriptase and an oligo (dT) primer. *E. coli* RNase H was used to nick the RNA in the RNA-DNA hybrid, and *E. coli* DNA polymerase replaced the RNA strand utilizing the nicked RNA as a primer (30). T4 DNA polymerase removed any remaining 3' overhangs from the first strand cDNA. ^{32}P dCTP was added to separate aliquots of the first and second strand cDNA synthesis reactions in order to analyze the reaction products (see Fig. 2). The cDNAs, which were not size fractionated, were inserted into λgt 10 at the Eco RI site which is located within the phage repressor gene (cI). The bacteriophages were packaged and used to infect NM514 (Amersham Corp., Arlington Heights, IL), an *E. coli* strain that contains a high frequency of lysogeny mutation (34). The library was screened by the "filter replica" method. Duplicate filters were made from each primary master plate so that spurious spots could be identified and ignored (4). The nylon filters (Micron Separations Inc., Westboro, MA) were hybridized at 68°C in 5× SSC (0.75 M NaCl, 75 mM sodium citrate, pH 7.0), 0.1% SDS, 5× Denhardt's reagent (0.1% ficoll, 0.1% polyvinylpyrrolidone, 0.1% BSA), 100 μg/ml denatured salmon sperm DNA, 10 mM EDTA in the presence of H$_4$, a 3' human IRBP cDNa generously provided by David C. Bridges, Gregory I. Liou, and Shao-Ling Fong (Baylor College of Medicine), which was labeled with ^{32}P by nick translation. The final posthybridization wash stringency was 1× SSC, 0.1% SDS at 45°C.

DNA Sequencing

Isolated rat IRBP cDNA fragments were subcloned into M13 and sequenced by the dideoxy chain termination method. Nested deletions were prepared by hybridizing an oligomer to the single-stranded M13 at the 3' end of the cloned insert, creating a double-stranded region at the Hind III site which was used to linearize the molecule (17). The 3' to 5' specific exonuclease activity of T4 DNA polymerase was exploited to digest varying amounts of the linearized DNA. The deletion products were tailed with dAs producing a short homopolymer tail at the 3' end which was used to anneal the two ends of the molecule. The remaining nick was sealed with T4 DNA ligase and the product used to transform competent JM109 *E. coli* cells (Stratagene Cloning Systems, La Jolla, CA).

Preparation of RNA

Eyes for the developmental studies were enucleated from Sprague-Dawley rats ranging in age from p0 (the day of birth) to p22. The lens was removed through a corneal incision except from p0 globes in order to avoid losing retinal tissue while removing the lens. This limited dissection avoids handling the delicate neonatal retina thus minimizing RNA degradation and optimizing quantitative recovery. The tissues were stored in 2.0-ml microfuge tubes in liquid nitrogen until use. The method of Chomczynski and Sacchi (16), which is well suited for quantitative extractions of total RNA from multiple small tissue samples, was modified as follows. 680 μl of 4 M guanidinium thiocyanate (Fluka Chemical Corp., Ronkonkoma, NY), 25 mM sodium citrate (pH 7), 0.5% sarcosyl, 0.1 M 2-mercaptoethanol was added to the frozen tissue which was immediately homogenized with a Polytron homogenizer fitted with a microgenerator probe (Brinkmann Instruments Co., Westbury, NY). The probe was then rinsed with an additional 200 μl of the above solution which was combined with the homogenate together with 57 μl of 3 M sodium acetate (pH 4.1), 833 μl of phenol (H$_2$O equilibrated), and 166 μl of chloroform/isoamyl (59:1). The mixture was shaken vigorously for 10 s, cooled on ice for 15 min, and centrifuged at 20,000 g for 30 min at 4°C. The RNA was precipitated from the supernatant with isopropanol and was dissolved in 200 μl of the quanidinium thiocyanate solution and quantitatively transferred to a 650-μl siliconized RNase free tube and again precipitated with isopropanol. The pellets, which were finally washed in 75% ethanol at −20°C and dried on a Speedvac concentrator (Savant Instruments, Inc., Hicksville, NY), dissolved readily in 25 μl H$_2$O that had been treated with diethyl pyrocarbonate (46). The concentration of RNA was determined using a scanning spectrophotometer (model DU-7; Beckman Instrument, Inc., Palo Alto, CA) and the OD$_{260}$/OD$_{280}$ ratio of the RNA ranged from 2.06 to 2.16.

RNA Probe

The RIa fragment was cloned into pGEM-4Z (Promega Biotec, Madison, WI) at the Eco RI site which is located in between Sp6 and T7 promoters. Because the insert contains SSp I sites located towards the 3' end and only one other SSp I site is present on the vector (see Fig. 2), the orientation of the insert was conveniently determined by the sizes of fragments produced by digestion with SSp I. The orientation of the probe was confirmed

by hybridizing the T7 and Sp6 run-off transcripts with blots of eye RNA (data not shown). To obtain a smaller insert, which would more easily generate full-length antisense transcripts for solution hybridization assays and be unique to the coding region, the noncoding 3' region was excised with Bam HI. The final probe termed rIRBPbe is shown in Fig. 1 and contains a 699-bp insert that corresponds to a coding sequence contained completely within the fourth repeat of the human IRBP gene. High specific activity antisense RNA probe was made by incubating 40 mM Tris-HCl (pH 7.5), 6 mM MgCl₂, 2 mM spermidine, 10 mM NaCl, 10 mM DTT, 500 μM ATP, 500 μM GTP, 500 μM CTP, 12 μM CTP, 0.05 μg/μl rIRBPbe linearized with Bgl II, 2.5 μCi/μl [α-³²P]-UTP, 0.5 U/μl T7 RNA polymerase at 37°C for 1 h.

Northern and Southern Blots

Both glyoxal and formaldehyde were used to denature RNA before electrophoresis in 1.4% Seakem GTG agarose (FMC, Rockland, ME) (46). The RNA was transferred to Nytran paper (Schleicher & Schuell, Inc., Keene, NH) and prehybridized at 68°C in 50% formamide, 5× Denhardt's reagent, 5× SSPE (1× SSPE is 0.18 M NaCl, 10 mM NaPO₄, pH 7.7, 1 mM EDTA), 0.5% SDS, and 100 μg/ml denatured salmon sperm DNA for 1–2 h. Hybridization was carried out at 68°C for 18 h in fresh buffer of the above composition which also contained 2 × 10⁶ cpm/ml of ³²P-labeled antisense IRBP RNA probe. The blots were then washed three times in 0.1× SSPE, 0.5% SDS at 68°C (15 min/wash), and exposed to XRP film (Kodak) with an intensifier screen (lightning plus; Dupont Co., Wilmington, DE) at −75°C. In the Northern blot of Fig. 5, Genescreen plus (Dupont Co.) paper was used and probed with the Rla cDNA fragment labeled with ³²P by nick translation (46). Prehybridization was carried out in 6× SSC (0.9 M NaCl, 135 mM sodium citrate, pH 7.0), 0.5% SDS, 5× Denhardt's solution, and 100 μg/ml denatured salmon sperm DNA at 68°C. The hybridization solution also included 0.01 M EDTA and 10⁶ cpm/ml of probe. The final wash stringency was 0.1× SSC (15 mM NaCl, 0.015 mM sodium citrate, pH 7.0), 0.5% SDS at 68°C.

Genomic DNA, isolated from the livers of male Sprague-Dawley rats (6), was digested and fractionated in 0.8% Seakem GTG agarose. After electrophoresis, the gel was incubated for 8 min in 0.25 N HCl, rinsed in H₂O, equilibrated in 0.4 M NaOH, 0.6 M NaCl, transferred to Nytran paper, neutralized in 0.5 M Tris (pH 7.0), 1 M NaCl, UV irradiated, and baked at 65°C. The blot was prehybridized in 6× SSPE, 10× Denhardt's reagent, 1% SDS, 50 μg/ml denatured salmon sperm DNA for 1.5 h at 60°C. Hybridization was carried out in 6× SSPE, 1% SDS, 50% formamide, 50 μg/ml denatured salmon sperm DNA, 5 × 10⁶ cpm/ml of ³²P-labeled antisense IRBP transcripts, at 60°C for 18 h. The blots were washed three times in 1× SSPE/1.0% SDS at 65°C for 15 min, once in 0.1× SSPE, 1.0% SDS for 20 min at 65°C, followed by 15 min in 2× SSC, 1 μg/ml RNase at 37°C.

Solution Hybridization Assays

The assay, adapted from Lee and Costlow (40) and Blum (7), consists of a series of hybridization reactions where increasing amounts of sample cellular RNA are mixed with 5 × 10⁴ cpm of antisense ³²P-labeled RNA probe. The amount of total RNA was set to 50 μg by the addition of yeast RNA. (The yeast RNA, obtained from Boehringer Mannheim Biochemicals, [Indianapolis, IN], was treated with proteinase K, extracted with phenol/chloroform, dialyzed against 10 mM Tris pH 7.0, 0.1 mM EDTA, ethanol precipitated, and redissolved in H₂O.) The above three components were precipitated with ammonium acetate, dried, and dissolved in 20 μl of 50% formamide, 0.4 M NaCl, 25 mM piperazine-N, N'-bis[2-ethanesulfonic acid] (pH 6.8), 1 mM EDTA, under 50 μl of mineral oil. The tubes were heated for 5 min at 85°C to ensure that the sample RNA and probe were fully denatured. Hybridization was carried out at 68°C for 18 h. Unhybridized probe was removed by RNase A and RNase T₁ which cleave 3' to pyrimidines and G residues, respectively. 300 μl of 0.05 U/ml RNase T₁ and 4.2 U/ml RNase A in 0.375 M NaCl, 0.075 M Tris (pH 8.0), 5 mM EDTA were added to each tube and incubated for 1 h at 37°C. While these two enzymes have a high specificity for single-stranded RNA, the optimum enzyme concentration was determined empirically in order to avoid nonspecific digestion of the RNA-RNA hybrid (see Fig. 8). After the RNase digestion, 300 μg of yeast RNA was added as carrier and each entire reaction immediately precipitated by the addition of an equal volume of ice-cold 10% (wt/vol) TCA. The precipitates were kept on ice for 10 min and collected on GF/C glass filters (Whatman Inc., Clifton, NJ). The radioactivity of the RNase resistant counts was determined by scintillation counting. Because the probe is in excess, a plot of radioactive probe contained in RNA
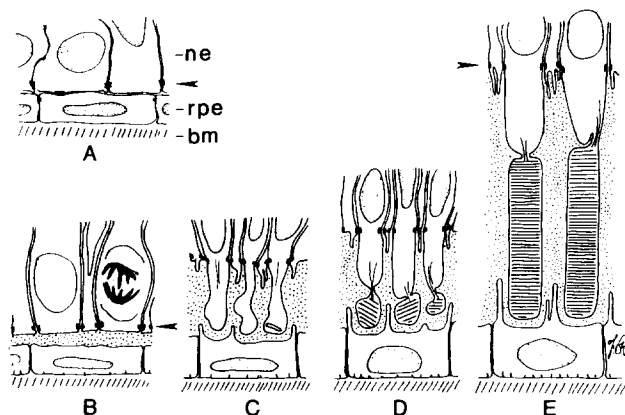

Figure 1. Development of the interphotoreceptor matrix in the rat. The invagination of the optic cup brings the neuroblastic epithelium (ne) in apposition with the retinal pigmented epithelium (rpe). Eventually, the cavity of the optic vesicle is obliterated by the formation of junctional complexes between these two cell layers (A). Shortly before birth, these complexes are released and the two layers separate. (B) At p0 (day of birth), the neural retina is separated from the RPE by a thin extracellular matrix (stippled area, not drawn to scale). (C) By p5, the interphotoreceptor matrix has greatly enlarged as inner segments protrude into the subretinal space. (D) At p10, primitive outer segments are present over most of the inner segments. (E) By p20, the outer segments have virtually achieved their adult length and the interphotoreceptor matrix has accumulated to accommodate the expanded volume of the subretinal space. Arrows in A, B, and E indicate the outer limiting membrane (tight junctions between photoreceptor and Muller cells). bm indicates the basement membrane of the RPE, Bruch's membrane.

duplex versus the input of cellular RNA is linear, and the amount of probe hybridized reflects the amount of cellular RNA used. The background hybridization is taken as the y intercept of this plot. The number of IRBP mRNA transcripts was determined from an internal calibration curve where known amounts of sense IRBP transcripts were hybridized with the ³²P antisense probe. Sense standard was synthesized by incubating Bam HI-linearized rIRBPbe probe (0.02 μg/μl) in 40 mM Tris-HCl (pH 7.5), 6 mM MgCl₂, 2 mM spermidine, 10 mM NaCl, 10 mM DTT, 1 U/μl RNasin (Promega Biotec), 0.5 mM each of ATP, CTP, GTP, and UTP, 0.1 U/μl SP6 RNA polymerase at 37°C for 60 min. The DNA template was removed with RQ1 DNase (Promega Biotec). The RNA standard was further purified by phenol/chloroform extraction, ethanol precipitation, and Sephadex G-50 spin column chromatography and its concentration measured spectroscopically. Determinations of the transcript prevalence using the internal standard agreed within experimental error to calculations based on the equation $T = nm/(\alpha\beta\delta)$, where T is the number of transcripts per microgram of total eye RNA, n is Avogadro's constant (6.023 × 10¹⁴ molecules/nmol), m is the experimentally determined slope of the titration curve, α is the ³²P fractional counting efficiency, β is the probe specific activity (dpm/ng), and δ is the molecular weight of the hybridizable portion of the probe (ng/mmol).

Results

150 positive clones were isolated from the rat neural retina cDNA library. One of these clones, termed R1, was purified to homogeneity. Eco RI digestion of the purified recombinant demonstrated two fragments, suggesting the presence of an internal Eco RI site (Fig. 2) which was confirmed by DNA sequencing. The two fragments Rla and Rlb, which had sizes of 1.3 and 0.9 kb, respectively, were subcloned into M13. The sequencing strategy is shown above the restriction map in Fig. 2. The coding region has a 83.9 and 82.5% nucleotide identity with the 3' end region of human and bo-
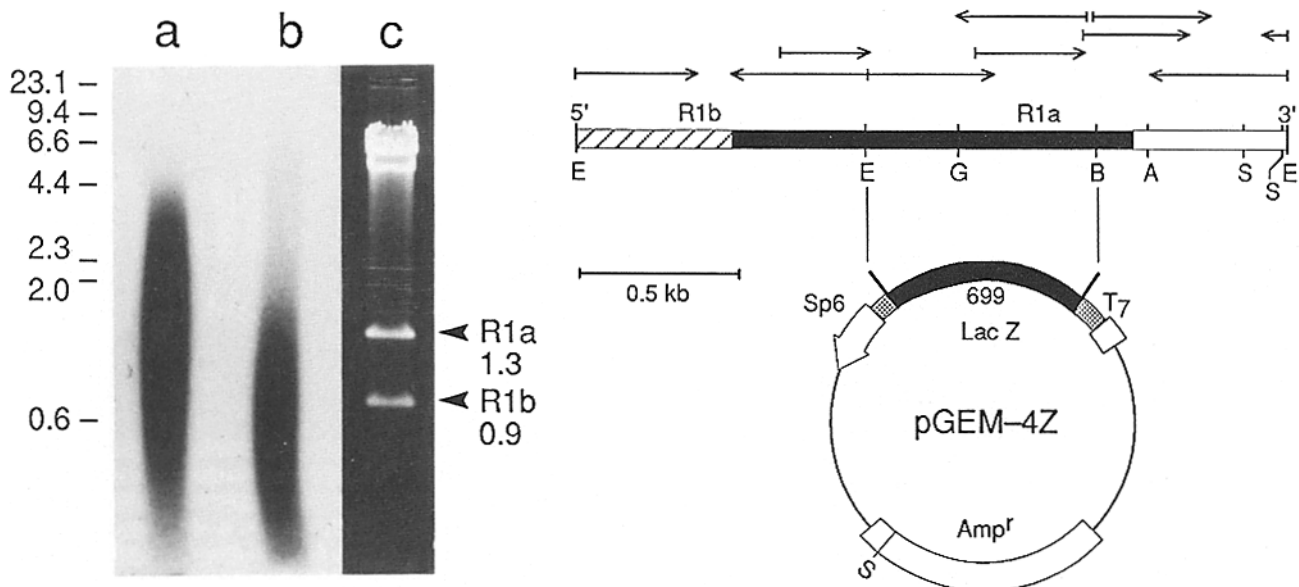
Figure 2. Molecular cloning of a rat IRBP cDNA and preparation of the rIRBPbe probe. (*left*) cDNA synthesis and isolation of a 2.2-kb clone. Lanes *a* and *b* are autoradiograms corresponding to the synthesis of first and second strand cDNA, respectively, from Sprague-Dawley neural retina poly (A) RNA. α ^{32}P-dCTP was incorporated into separate aliquots of the reactions in order to analyze the products of 1.4% agarose gel electrophoresis. The cDNAs were cloned into the Eco RI site of lambda gt10 and the resulting library was screened with a human IRBP 3' cDNA. Lane *c* is an ethidium bromide–stained gel of a purified recombinant digested with Eco RI. (*right*) Restriction map of the rat IRBP cDNA which consists of an open reading frame (*solid*) followed by 3' noncoding sequence (*open*). The hatched 5' end represents ligation artifact during the preparation of the library. The sequencing strategy is summarized above the restriction map. A 699-bp Eco RI–Bam HI fragment was subcloned in between the Sp6 and T7 promoters of pGEM-4Z. *E*, Eco RI; *G*, Bgl II; *B*, Bam A and/or T$_1$; (●) RNase T$_1$;

vine IRBP, respectively. The rat clone corresponds to a sequence contained entirely within the fourth repeat of the gene sequence of human and bovine IRBP (8, 15, 25, 45, 53). The translated amino acid sequence of the rat IRBP clone shows virtually conservative substitutions when compared to the known amino acid sequences of bovine IRBP cyanogen bromide peptide fragments. The open reading frame terminates with a TAG codon which is followed by nontranslated 3' sequence ending in 10 adenosine residues. Although an A-T-rich sequence (AATATT) precedes the poly A region by 22 residues, a signal sequence is not present. The 5' portion of the cloned insert, which shows no homology with either the sequence of bovine or human IRBP, represents DNA artifactually introduced into this clone during the ligation step of the cDNA library preparation.

Based on this characterization of the R1 cDNA clone, an Eco RI–Bam HI fragment 699 bp in length containing only coding sequence was selected for the preparation of the RNA probe used in this study. This fragment was subcloned in between the Sp6 and T7 promoters of pGEM-4Z as shown in Fig. 2. The final construct termed rIRBPbe, can be conveniently linearized with Bgl II in order to generate antisense probe off the T7 promoter. The nucleotide sequence immediately 3' to the Bgl II site is given in Fig. 3. An alignment to the corresponding region of human IRBP sequence is included in the figure.

Fig. 4 shows that two forms of the mRNA for IRBP exist in the rat eye. The doublet in the autoradiogram in lane *c* consists of a major species 5.2 kb in size and a less abundant transcript of 6.4 kb. Laser densitometry demonstrated that the two transcripts are present in a 4:1 ratio, respectively.

The autoradiograms were scanned at different band intensities in order to ensure that the densitometric measurement was performed in the linear response region of the photographic emulsion. A side-by-side comparison of the rat IRBP doublet with bovine IRBP mRNA is shown in Fig. 5. The mRNA for bovine IRBP consists of a single species which corresponds in size to the larger form of the rat IRBP mRNA. Although 2 μg of poly(A$^+$) RNA was loaded in each lane, the bovine band is markedly fainter than the rat doublet because high stringency conditions were used. When an identical blot was probed with B23, a bovine IRBP cDNA (43) under the same conditions, the bovine band was more intense than the rat doublet (data not shown). This indicates that the rat IRBP probe is less sensitive for bovine IRBP mRNA due to the partial homology of the IRBP mRNAs between these two species. Rat genomic DNA was digested with Eco RI, Hind III, Bgl II, and Sac I. The Southern blot in Fig. 6 shows only one band in each of the four lanes.

In Fig. 7, 10 μg of total RNA extracted from globes enucleated from rats ranging in age from p0 to p20 was subjected to Northern blot analysis. Before transfer, the gel was stained with acridine orange and photographed under ultraviolet light (Fig. 7 *B*) confirming that equivalent amounts of RNA were present in each lane and that the RNA was not degraded. The RNA from the same gel was blotted to Nytran paper and probed with the ^{32}P-labeled rat IRBP antisense RNA (Fig. 7 *A*). The 5.2/6.4-kb doublet, indicated by the lower pair of arrows in Fig. 7 *A*, is not well resolved due to the high loading level of RNA in the gel and distortion created by the larger ribosomal subunit band which has a similar electrophoretic mobility as the IRBP bands. A faint band of

```
ACAACCGGCCCAACGACTCGATGAGGGAACTTTGGACACACTCGCAGCTCACAGGTGAA
::: :::::: : ::::: : :: ::::: ::::::::::: : ::: :    :::::::
ACAGCCGGCCTGATGACTCTGTCAGTGAACTCTGGACACACGCCCAGGTTGTAGGTGAA


CGATATGGCTCCAAGAAGAGTGTAGCCATCCTGACCAGCGGTGTGACAGCCGGCGCCGCC
:: :::::::::::::::::: : : ::: :::::::::: :::::: :::::: ::::
CGCTATGGCTCCAAGAAGAGCATGGTCATTCTGACCAGCACTGTGACGGCCGGCACCGCG


GAGGAATTTACTTACATCATGAAGAGGCTGGGCCGGGCCCTGGTCGTTGGTGAAGTGACA
::::: :: :: :: ::::::::::::::::::::::::::::::: :::: :: :::::
GAGGAGTTCACCTATATCATGAAGAGGCTGGGCCGGGCCCTGGTCATTGGGGAGGTGACC


AGTGGAGGCTGCCAGCCACCACAGACCTACCACGTGGACGACACGCATCTCTATATCACC
::::: :::::::::::::::::::::::::::::::::: ::::: : ::::: ::::
AGTGGGGGCTGCCAGCCACCACAGACCTACCACGTGGATGACACCAACCTCTACCTCACT


ATCCCCACAGCTCGCTCTGTGGGCGCCACGGACGGCAGTTCCTGGGAAGGGGTGGGTGTG
:::::::::: :: :: ::::::::: ::: :::: ::::: ::::::::::::::::: : :
ATCCCCACGGCCCGTTCTGTGGGGGGCCTCGGATGGCAGCTCCTGGGAAGGGGTGGGGGTG


ACACCTAATGTAGTTGTCTCTTCAGAATTGGCTCTTACCAGAGCCAAGGAGATACTCCAG
::::: :::: :::::: :: ::::: :::::: :::: :::::::::: ::::::
ACACCCCATGTGGTTGTCCCTGCAGAAGAGGCTCTCGCCAGGGCCAAGGAGATGCTCCAG
```
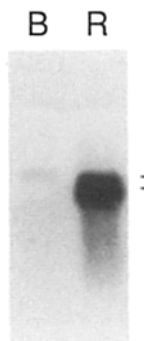
Figure 3. Nucleotide sequence of the rat IRBP RNA probe (*upper sequence*) used for the majority of the experiments in this paper. The sequence begins immediately 5' to the Bgl II site of the cloned insert in Fig. 2. The lower strand is an alignment of the corresponding sequence of human IRBP. These sequence data are available from EMBL/GenBank/DDBJ under accession number X56159.

Figure 5. Northern blot autoradiogram comparing bovine (B) and rat (R) IRBP mRNAs. The bovine IRBP mRNA has a similar electrophoretic mobility as the larger form of the mRNA of rat IRBP. 2 μg of neural retina poly (A) RNA was loaded in each lane. The blot was probed with the rla fragment of the rat IRBP cDNA clone under high stringency conditions. The bovine band is faint because of the partial homology between the bovine and rat IRBP mRNAs. Arrowheads correspond to 6.4 and 5.2 kb.

~10 kb is indicated by the upper arrowhead in this panel. This band is frequently observed in overexposed Northern blot autoradiograms. The mRNA for IRBP in the postnatal rat eye was easily demonstrated at p0 (the day of birth). However, it is not clear whether both forms of the message are present at p0–p3. Whether the two forms of the mRNA for IRBP are differentially expressed during development will have to await further study. In any event, the quantity of both
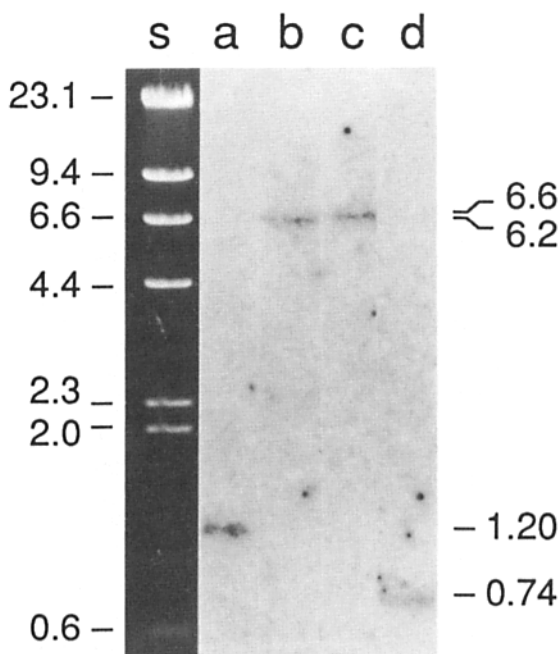
IRBP mRNAs increases rapidly during the first week of life with the adult level of expression being reached by p9.

To obtain quantitative measurements of the expression of the mRNA for IRBP during development, a solution hybridization assay was employed to determine the number of IRBP mRNA transcripts/microgram total RNA. Figs. 2 and 3 characterize the assay. The validity of the assay depends on the satisfaction of three criteria. (*a*) The antisense RNA probe should be in 10-fold excess of target. (*b*) The sense and antisense transcripts should be full length. This is an important point because some eukaryotic sequences act as efficient stop signals for phage RNA polymerases (40). (*c*) The minimum amount of RNase required to digest the unhybridized probe should be determined in order to avoid nonspecific digestion of the RNA–RNA hybrid. Conditions of excess probe were determined by measuring the RNase resistant

Figure 4. Northern blot analysis of rat IRBP mRNA. (*left*) An ethidium bromide–stained 1% agarose gel showing molecular weight standards in kb (lane *a*) and ribosomal subunits (lane *b*). Lane *c* is the autoradiogram of the Northern blot probed with ³²P-labeled antisense rat IRBP transcripts. 5 μg of total eye RNA was loaded in lanes *b* and *c*. (*right*) The IRBP mRNA doublet consists of a major species of 5.2 kb and a less abundant transcript of 6.4 kb. A laser densitometric scan of the doublet is shown in the insert. The scan was taken at an exposure density corresponding to the linear response range of the photographic emulsion.

Figure 6. Southern blot autoradiogram of rat genomic DNA. 5 μg of liver Sprague-Dawley genomic DNA was digested with (lane *a*) Eco RI; (lane *b*) Hind III; (lane *c*) Bgl II; and (lane *d*) Sac I. The blot was probed with ³²P-labeled antisense IRBP RNA probe as described under Materials and Methods. Lane *s* is the ethidium bromide–stained Hind III fragments of lambda phage DNA. Size markers are in kb.
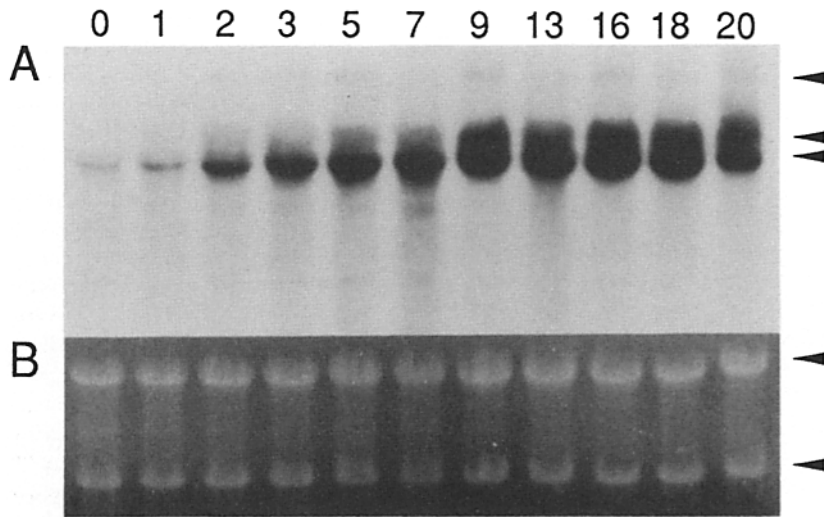
Figure 7. Expression of the mRNA for IRBP during development in the rat. Numbers above the lanes correspond to the postnatal age (p0 is the day of birth). 10 μg of total eye RNA were loaded in each lane. *B,* which shows the gel stained with acridine orange before blotting, confirms that the loading levels for each lane were equivalent. *A* is the autoradiogram of the blot probed with ^{32}P-labeled antisense IRBP transcripts.

TCA precipitable counts at increasing concentrations of input cellular RNA. Only the initial linear region was used for calculations of the slope. The insert of Fig. 8 is a Northern blot that demonstrates that both the sense and antisense transcripts are virtually full length. Finally, the optimum concentrations of RNase A and RNase T_1 were determined empirically by separately titrating each of the two enzymes as shown in Fig. 8. From the data presented in this figure, the concentration of RNase A and RNase T_1 were selected to be 4.2 and 83 U/ml, respectively. This pair of enzyme concentrations results in digestion of ~99.5% of unhybridized ^{32}P antisense probe after a 1-h incubation at 37°C.

Fig. 9 demonstrates that the assay is not only remarkably sensitive but also is linear over a wide range of target sense RNA concentrations. 2–750 pg of sense transcripts generated from the rIRBPbe probe linearized with Bam HI, were incubated as described under Materials and Methods with 5 × 10⁴ cpm of ^{32}P-labeled antisense IRBP RNA. The samples were then treated with RNases A and T_1 and the RNase resistant TCA precipitable RNA–RNA hybrids were collected on glass filters and their radioactivity was determined by scintillation counting. Standard calibration curves such as the one in this figure were included in all assays and the determination of the number of IRBP transcripts was
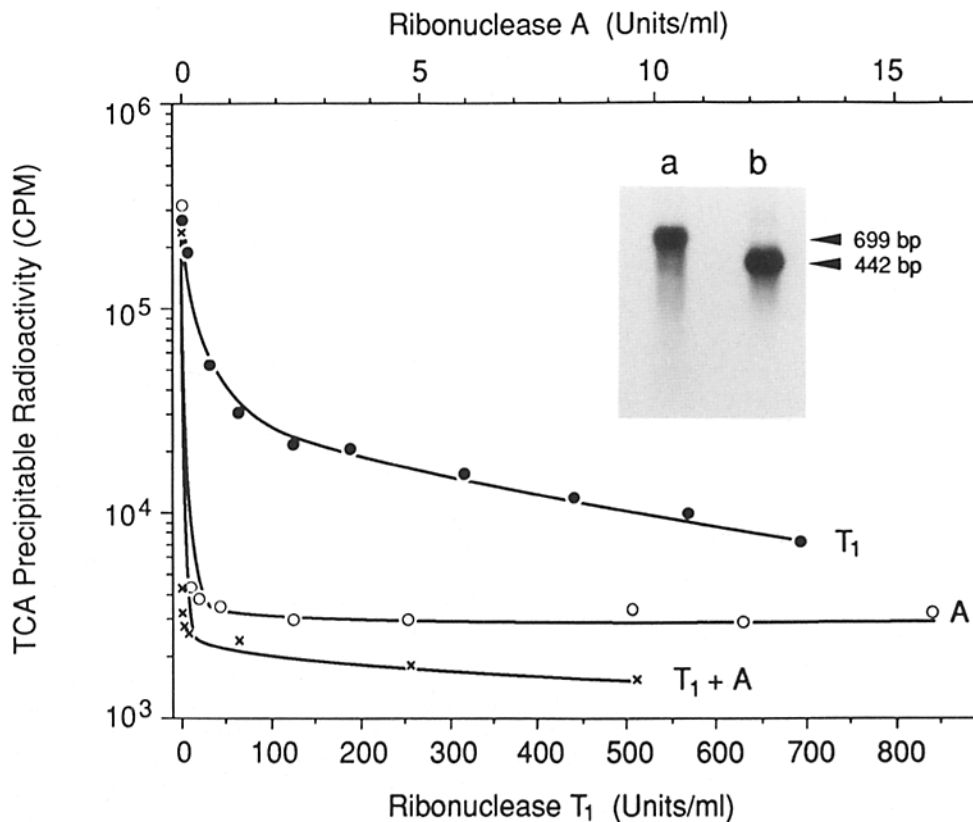
Figure 8. Characterization of the solution hybridization assay used to measure the quantity of the mRNA for IRBP. The optimum concentrations of RNase A and T_1 were determined by enzyme titration. ^{32}P-labeled antisense IRBPb transcripts were incubated at 37°C for 1 h in the presence of varying concentrations of RNase A and/or T_1; (●) RNase T_1; (○) RNase A; and (×) RNase A and T_1. The insert is an autoradiogram of a Northern transfer which demonstrates that the ^{32}P-labeled sense (lane *a*) and antisense (lane *b*) transcripts generated using the Sp6 and T7 promoters, respectively, of the rIRBPbe construct are virtually full length. The sense probe was linearized with Bam HI and the antisense probe with Bgl II (see Fig. 1). The RNA for the Northern blot was fractionated in 1.4% agarose.
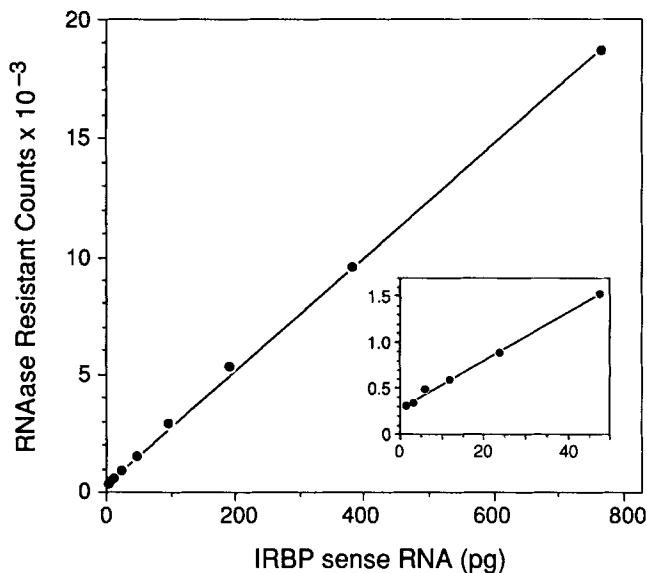
Figure 9. Solution hybridization assay demonstrating a linear relationship between the level of RNase resistant counts versus the amount of target sense transcripts over a range of 3–800 pg. Sense transcripts were generated off the Sp6 promoter using the rIRBPbe probe linearized with Bam HI while antisense probe was generated off the T7 promoter with Bgl II-linearized probe. Sense transcripts were hybridized to the ^{32}P-labeled antisense probe and treated with RNase A and T_1. The RNase-resistant counts were then collected on glass filters and the radioactivity was determined by scintillation counting.

based on the internal calibration curve. To check the accuracy of this method, a theoretical calculation of transcript prevalence was also performed where the number of IRBP mRNA molecules was determined from the TCA precipitable RNase resistant radioactivity, by applying Avogadro's number, the specific activity and length of the RNA probe, and the counting efficiency of the scintillation counter. The two methods agreed, within experimental error, on the value for IRBP mRNA prevalence.

The above solution hybridization assay was used in Fig. 10 to determine the number of IRBP mRNA molecules in the retina during postnatal eye development. The number of transcripts is expressed per microgram of total eye RNA. The insert of this figure provides the relationship between the level of total eye RNA and the postnatal age. Approximately 10^5 IRBP transcripts/μg total RNA (or 10^6 transcripts/eye, see Fig. 11) are present at birth in the rat eye. By p9 the level of the mRNA for IRBP has reached a plateau of 3.1 × 10^6 transcripts/μg total RNA (9 × 10^7 transcripts/eye). One-half of the maximal expression of the mRNA for IRBP is reached at p4.2.

Discussion

Because of its strategic position between the RPE and the neural retina, early investigators have proposed that the function of the interphotoreceptor matrix is to facilitate diffusion of nutrients across the subretinal space to the photoreceptors (61). This concept is being supported by mounting evidence that the function of IRBP is to facilitate the diffusion of vitamin A through the hydrophilic domain of the

interphotoreceptor matrix during the visual cycle in the adult retina (12, 37, 38, 41, 42, 47, 51, 57). While IRBP is therefore critical to visual function in the mature retina, this protein has been demonstrated in the mouse eye by Western blot at gestational age E17 (14), an age where the visual cycle is probably not physiologically significant (10, 14). In the human fetus, IRBP has been found by immunocytochemistry at 20 wk gestation (36). The function of IRBP at these early stages of eye development has not been determined.

Quantitative measurements employing densitometric scanning of Coomassie blue–stained SDS-PAGE gels, ELISA, and rocket immunoelectrophoresis (14, 20, 26, 28) have shown that the amount of IRBP in the subretinal space of mice and rats rises rapidly between p10 and p25 in parallel with the quantity of rhodopsin. The quantity of IRBP in the subretinal space is determined by the rate of its secretion by the photoreceptors and the rate of its removal from the extracellular compartment. Little is known concerning how IRBP is removed from the subretinal space (possible mechanisms are summarized in ref. 29). Hollyfield et al. (33) have obtained evidence that the rod and cone photoreceptors internalize and degrade IRBP. Since nothing is known regarding the kinetics of IRBP turnover in the subretinal space, it is not clear whether the accumulation of IRBP during development directly reflects the expression of the IRBP gene. For example, if IRBP is only slowly removed from the subretinal space, the increase in quantity of IRBP that occurs between p10 and p25 may reflect the protein accumulating in the interphotoreceptor matrix as the subretinal space expands with the elongation of the rod outer segments. To better understand the dynamics of the production of this important extracellular matrix we wanted to measure the expression of the mRNA for IRBP during the ontogeny of the retina.

A rat retina cDNA library was prepared from which an IRBP clone was obtained by low stringency screening. The isolation of a rat-specific IRBP clone has allowed us to perform quantitative measurements of IRBP transcript preva-
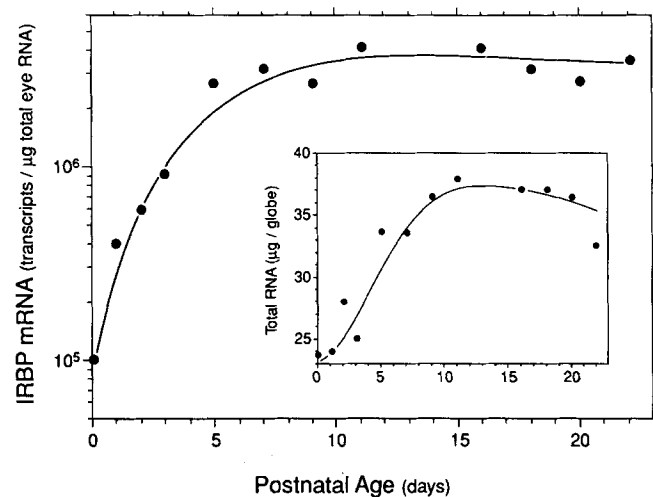
Figure 10. Expression of the mRNA for IRBP during photoreceptor differentiation. The number of IRBP mRNA transcripts, determined by solution hybridization assay, was divided by the amount of total RNA. The insert demonstrates the relationship between the amount of total RNA/eye and the postnatal age.
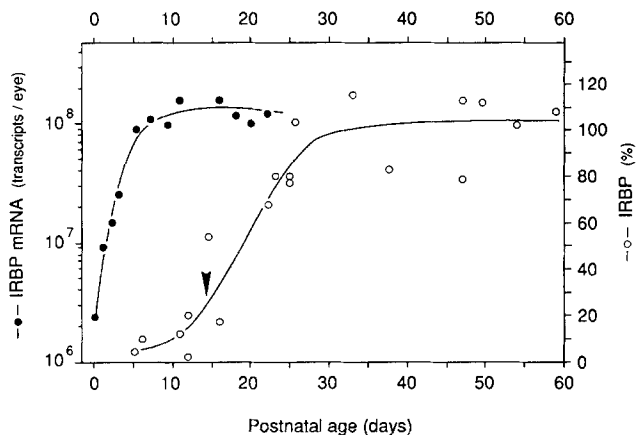
Figure 11. Comparison of the expression of IRBP and its mRNA at different postnatal ages. (●) number of IRBP mRNA transcripts/eye; (○) quantity of IRBP in the subretinal space/eye (arbitrary units). The protein levels, determined by laser densitometry of the Coomassie blue-stained IRBP band in SDS polyacrylamide gradient gels, is here reploted from Gonzalez-Fernandez et al. (26). Arrow indicates p14, the age of eye opening.

lence. The relatively high degree of sequence homology between the isolated rat IRBP cDNA and the known nucleotide sequence of human and bovine IRBP confirms the authenticity of the recombinant clone. While the clone ends in 10 adenosine residues, it is unlikely that this represents the 3' end of the mRNA since the poly A region is not preceded by a signal sequence. Furthermore, since the mRNA of rat IRBP is similar in size to human and bovine IRBP mRNAs, the length of the two forms of the mRNA for rat IRBP predicts that the 3' noncoding region should extend beyond the present sequence data. The existence of two forms of the message for IRBP may be unique to the rat and the sizes of the transcripts (6.4 and 5.2 kb) are similar to that reported by others (35). The large 6.4-kb form is virtually identical in size to the mRNA of bovine IRBP. A faint band is sometimes seem at ~10 kb which may represent a nuclear precursor. In mouse, hamster, and rabbit, Inouye et al. (35) have observed less abundant higher molecular weight bands. These workers have also observed second lower molecular weight bands in hamster and bovine retina but are cautious in the interpretation of these putative bands because of the possibility of tailing of the IRBP mRNA signal and the presence of a large amount of 28s ribosomal RNA nearby. The two forms of the mRNA for IRBP were found not only in the Sprague-Dawley rat but were also present in Wistar rats as well as in the Royal College of Surgeon pink eye controls, indicating that the finding is not unique to a particular strain of rat. The presence of two IRBP mRNAs in rat may be explained by an unprocessed nuclear precursor, alternative splicing of the mRNA, or usage of alternative adenylation sites in the 3' nontranslated region. Our genomic Southern blot data suggests that only one allele of the gene for IRBP exists in the rat. The explanation for the two IRBP mRNAs in rat probably lies in the 3' nontranslated region. The smaller size of the human IRBP mRNA compared to the bovine transcript is due to loss by the human gene of a 1.7-kb segment of DNA between the translation termination codon and the 3'-AAT-AAA consensus sequence (25). The multiple forms of mouse

and rat opsin mRNAs have recently been shown to be due to the selective use of polyadenylation sites present in the 3' untranslated region (Baehr, W., S. J. Pittler, M. Champagne, and M. R. Al-Ubaidi. 1990. *Invest. Ophthalmol. & Visual Sci.* 31:75). We are presently studying additional IRBP cDNA clones in order to understand the origin of the two forms of the mRNA for this protein in the rat retina.

We have studied the expression of the mRNA for IRBP during photoreceptor differentiation by two independent techniques, Northern blot analysis and molecular titration assay. To maximize the accuracy of the measurements, we avoided dissecting the retina from the eye and removed only the lens through a slit in the cornea. The advantage of this limited dissection is that the delicate neonatal retina is not disturbed, minimizing RNA degradation and optimizing the quantitative recovery of the tissue. It should be kept in mind that since we are expressing the number of mRNA molecules for IRBP in terms of total eye (minus lens) RNA, we are assuming that the amount of photoreceptor RNA during development increases proportionally with the quantity of non-photoreceptor RNA. While this is approximately correct since the photoreceptors make up the majority of the retinal neurons and the nonretinal ocular structures enlarge during development proportionally to the enlargement of the retina, studies using multiple photoreceptor specific markers are now in progress in our laboratory. To correct for changes in the amount of total RNA with age and variability in the RNA extraction, equivalent amounts of total RNA were loaded in each of the lanes in the Northern blot of Fig 7 and the IRBP transcript prevalence was expressed per microgram total RNA in Fig. 10. Northern blot analysis and the solution hybridization assay demonstrated the same pattern of expression of the IRBP mRNA. The message was easily detected at p0 by Northern blot, and 10^5 transcripts/μg total RNA were measured by solution hybridization. The mRNA level reached a plateau of 3.1×10^6 transcripts/μg RNA at p9. The one-half maximal level of expression (1.55×10^6 transcripts/μg RNA) was reached at p4.2. This early pattern of expression for the mRNA of IRBP is in contrast to the pattern of expression of the quantity of IRBP in the subretinal space. Fig. 9 compares the expression of mRNA for IRBP with measurements of the amount of IRBP in the subretinal space replotted from Gonzalez-Fernandez et al. (26). These investigators determined the level of IRBP by laser densitometry of the Coomassie blue–stained IRBP band on SDS-PAGE gels of rat interphotoreceptor matrix. The quantity of IRBP rises rapidly between p10 and p25 reaching a plateau by p30. The emergence of rhodopsin is virtually identical to the pattern of expression of IRBP.

The expression of IRBP is different than that of its mRNA. The level of the mRNA for IRBP reaches a plateau at p9, ~3 wk before the protein achieves adult levels in the matrix. While we initially expected that the message and protein levels would have the same pattern of expression, an explanation for the difference can be offered from morphologic observations of the developing retina (21, 59). The interphotoreceptor matrix, which is present at birth in rodents, undergoes marked changes in its proportions during postnatal development as the inner segments and later the outer segments protrude into the subretinal space (Fig. 1). By p5 the extracellular space between the RPE and external limiting membrane has greatly expanded due to extension of the inner segments

into the subretinal compartment. With the emergence of outer segments during the next 2 wk of life, the subretinal space continues to expand as the external limiting membrane and apical surface of the pigmented epithelium become further separated. During this time, the various components of the interphotoreceptor matrix must be rapidly added to the subretinal space to compensate for its increasing volume. Thus, a possible explanation for the discrepancy between the emergence of IRBP and the expression of its mRNA is that the protein is steadily accumulating in the extracellular compartment although the rate of its synthesis is constant.

Regulation of gene expression during development may occur at the level of synthesis, processing, destruction of mRNA, or a combination of these mechanisms. The observed increase in quantity of the mRNA for IRBP is at least in part due to an enhancement in synthesis, since a fivefold increase in the rate of transcription of the IRBP gene occurs between p1 and p9 in the rat (55). If the rate of degradation of the IRBP mRNA is constant, a fivefold increase in transcription would predict that the level of this mRNA should also increase fivefold. Since the level of IRBP mRNA rises ~30-fold during this period, an increase in mRNA stability may also be contributing to the rapid accumulation of IRBP transcripts during development. Interestingly, the mRNAs for IRBP and the alpha subunit of phosphodiesterase appear to be more stable than the mRNAs for S-antigen and the alpha subunit of transducin in both the adult and developing bovine retina (Hauswirth, W. W., L. E. DesJardin, L. Morel, and A. M. Timmers. 1990. *Invest. Ophthalmol. & Visual Sci. Suppl.* 31:159).

Since the visual cycle is probably not physiologically significant during early retinal development, the high expression of the mRNA for IRBP during the first postnatal week and the ability of others to detect IRBP at E17 (14) in the mouse and at 20 wk gestation in man (36), suggests that IRBP may have a different function during this period of time. As discussed above, IRBP may have a general role in facilitating the diffusion of hydrophobic nutrients to the neural retina. More specifically, IRBP may be involved in the transport of morphogens, possibly vitamin A, to the neuroblastic epithelium. Retinoids, which are potent teratogens, have been implicated as endogenous morphogens during development. The study of the spatial and temporal pattern of the expression of the mRNA for cellular retinoic acid–binding protein and cellular retinol–binding protein during mouse embryogenesis has shed light on the function of these vitamin A binding proteins during development (18, 48). Tissues that are known to be teratogenic targets of retinoic acid and retinol also express CRABP and CRBP transcripts. In the embryonic mouse, CRABP is expressed in the retinal layer and CRBP is expressed in both the retinal and pigmented epithelial layers. IRBP, the protein believed to transport vitamin A between these two layers, is also present in the embryonic mouse eye (14) which is at least consistent with the hypothesis that these proteins may participate in the establishment of a vitamin A gradient in the retina during ocular embryogenesis. The fact that the quantity of IBRP in the subretinal space is not very high during the early postnatal period does not necessarily diminish its importance as a transport vehicle. Since the volume of the subretinal space is smaller at this time and the apical surface of the RPE is much closer to the outer nuclear layer, less IRBP would be needed to accomplish the task of facilitating the diffusion of hydrophobic molecules to the neural retina.

In conclusion, we have used the expression of the mRNA for IRBP as a marker for the synthesis of interphotoreceptor matrix. The surprising early expression of the mRNA during postnatal eye development is consistent with the idea that this extracellular matrix may have an important role in transporting hydrophobic nutrients from the choroid capillaris/RPE complex to the growing and differentiating neural retina.

References

1. Adler, A. J., W. F. Stafford, and H. S. Slayter. 1987. Size and shape of bovine interphotoreceptor retinoid-binding protein by electron microscopy and hydrodynamic analysis. *J. Biol. Chem.* 262:13189–13203.
2. Angerer, L. M., K. H. Cox, and R. C. Angerer. 1987. Molecular titration assay to measure transcript prevalence levels. *Methods Enzymol.* 152: 633–648.
3. Baazan, N. G., T. S. Reddy, T. M. Redmond, B. Wiggert, and G. J. Chader. 1985. Endogenous fatty acids are covalently and noncovalently bound to interphotoreceptor retinoid-binding protein in the monkey retina. *J. Biol. Chem.* 260:13677–13680.
4. Berger, S. L., and A. R. Kimmel. 1987. Guide to Molecular Cloning Techniques. *Methods Enzymol.* Vol. 152.
5. Bernstein, P. S., W. C. Law, and R. R. Rando. 1987. Isomerization of all-trans-retinoids to 11-cis-retinoids *in vitro. Proc. Natl. Acad. Sci. USA.* 84:1849–1853.
6. Blin, N., and D. W. Stafford. 1976. Isolation of high molecular weight DNA. *Nucleic Acids Res.* 3:2303–2308.
7. Blum, M. 1989. Regulation of neuroendocrine peptide gene expression. *Methods Enzymol.* 168:618–633.
8. Borst, D. E., T. M. Redmond, J. E. Elser, M. A. Gonda, B. Wiggert, G. J. Chader, and J. M. Nickerson. 1989. Interphotoreceptor retinoid-binding protein: gene characterization, repeat structure, and its evolution. *J. Biol. Chem.* 264:1115–1123.
9. Bowes, C., T. Van Veen, and D. B. Farber. 1988. Opsin, G-protein and 48-kDa protein in normal and rd mouse retinas: developmental expression of mRNAs and proteins and light/dark cycling of mRNAs. *Exp. Eye Res.* 47:369–390.
10. Bridges, C. D. B. 1989. Distribution of retinol isomerase in vertebrate eyes and its emergence during retinal development. *Vision Res.* 29:1711–1717.
11. Bridges, C. D. B., and R. A. Alvarez. 1987. The visual cycle operates via an isomerase acting on all-trans retinol in the pigment epithelium. *Science (Wash. DC).* 236:1678–1680.
12. Bridges, C. D. B., R. A. Alvarez, S.-L. Fong, F. Gonzalez-Fernandez, D. M. K. Lam, and G. I. Liou. 1984. Visual cycle in the mammalian eye: retinoid-binding proteins and the distribution of II-cis retinoids. *Vision Res.* 24:1581–1594.
13. Bridges, C. D. B., G. I. Liou, F. Gonzalez-Fernandez, R. A. Alvarez, and S.-L. Fong. 1988. Vitamin A: utilization, metabolism, and role in retinal disease. *In* Retinal Diseases: Biomedical Foundations and Clinical Management. MOM Isu, editor. J. B. Lippincott. 49–59.
14. Carter-Dawson, L., R. A. Alvarez, S.-L. Fong, G. I. Liou, H. G. Sperling, and C. D. B. Bridges. 1986. Rhodopsin, 11-cis vitamin A, and interstitial retinol-binding protein (IRBP) during retinal development in normal and rd mutant mice. *Dev. Biol.* 116:431–438.
15. Chader, G. J. 1989. Interphotoreceptor retinoid-binding protein (IRBP): a model for molecular biological and clinically relevant studies. *Invest.*

Ophthalmol. & Visual Sci. 30:7-22.

16. Chomczynski, P., and N. Sacchi. 1987. A rapid method of RNA isolation by acid guanidinium thiocyanate-phenol-chloroform extraction. *Anal. Biochem.* 162:156-159.

17. Dale, R. M. K., and A. Arrow. 1987. A rapid single-stranded cloning, sequencing, insertion, and deletion strategy. *Methods Enzymol.* Inc. 177:204-214.

18. Dolle, P., E. Ruberte, P. Kastner, M. Petkovich, C. M. Stoner, L. J. Gudas, and P. Chambon. 1989. Differential expression of genes encoding alpha, beta, and gamma retinoic acid receptors and CRBP in the developing limbs of the mouse. *Nature (Lond.).* 342:702-703.

19. Eisenfeld, A. J., A. H. Bunt-Milam, and J. C. Saari. 1985. Immunocytochemical localization of interphotoreceptor retinoid binding protein in developing normal and RCS rat retinas. *Invest. Ophthalmol. & Visual Sci.* 26:775-778.

20. Ekstrom, P., B. Wiggert, L. Lee, Y. Hiroso, S. Sanyal, and G. J. Chader. 1988. A developmental study of interphotoreceptor retinoid-binding protein (IRBP) in single and double homozygous rd and rds mutant mouse retinae. *Exp. Eye Res.* 47:291-305.

21. Feeney, L. 1973. The interphotoreceptor space I. Postnatal ontogeny in mice and rats. *Dev. Biol.* 32:101-114.

22. Fisher, S. K., and K. A. Linberg. 1975. Intercellular junctions in the early human embryonic retina. *J. Ultrastruct. Res.* 51:69-78.

23. Fong, S.-L., G. I. Liou, R. A. Landers, R. A., Alvarez, F. Gonzalez-Fernandez, P. A. Glazebrook, D. M. K. Lam, and C. D. B. Bridges. 1984. Characterization, localization and biosynthesis of an interstitial retinol-binding glycoprotein in the human eye. *J. Neurochem.* 42:1617-1676.

24. Fong, S.-L., G. I. Liou, R. A. Landers, R. A. Alvarez, and C. D. B. Bridges. 1985. Purification and characterization of a retinol-binding glycoprotein synthesized and secreted by bovine and neural retina. *J. Biol. Chem.* 259:6534-6542.

25. Fong, S.-L., W.-B. Fong, T. A. Morris, K. M. Kedzie, and C. D. B. Bridges. 1990. Characterization and comparative structural features of the gene for human interstitial retinol-binding protein. *J. Biol. Chem.* 265:3648-3653.

26. Gonzalez-Fernandez, F., R. A. Landers, P. A. Glazebrook, S.-L. Fong, G. I. Liou, D. M. K. Lam, and C. D. B. Bridges. 1984. An extracellular retinol-binding glycoprotein in the eyes of mutant rats with retinal dystrophy: development, localization and biosynthesis. *J. Cell Biol.* 99:2092-2098.

27. Gonzalez-Fernandez, F., R. A. Landers, P. A. Glazebrook, S.-L. Fong, G. I. Liou, D. M. K. Lam, and C. D. B. Bridges. 1985. An extracellular retinol-binding glycoprotein in the rat eye-characterization, localization and biosynthesis. *Neurochem. Int.* 7:533-540.

28. Gonzalez-Fernandez, F., S.-L. Fong, G. I. Liou, and C. D. B. Bridges. 1985. Interstitial retinol-binding protein (IRBP) in the RCS rat: effect of dark-rearing. *Invest. Ophthalmol. & Visual Sci.* 26:1381-1385.

29. Gonzalez-Fernandez, F., R. A. Landers, S.-L. Fong, G. I. Liou, and C. D. B. Bridges. 1985. Interstitial retinol-binding protein in the interphotoreceptor matrix of normal and dystrophic rats. *In* The Interphotoreceptor Matrix In Health and Disease. CDB Bridges and AJ Alder, editors. Alan R. Liss, Inc., New York. 213-229.

30. Gulber, U. 1987. Second-strand cDNA synthesis: mRNA fragments as primers. *Methods Enzymol.* 152:330-335.

31. Ho, M.-T. P., J. B. Massey, H. J. Pownall, R. E. Anderson, and J. G. Hollyfield. 1989. Mechanism of vitamin A movement between rod outer segments, interphotoreceptor retinoid-binding protein, and liposomes. *J. Biol. Chem.* 264:928-935.

32. Hollyfield, J. G., S. J. Fliesler, M. E. Rayborn, S.-L. Fong, R. A. Landers, and C. D. Bridges. 1985. Synthesis and secretion of interstitial retinol-binding protein by the the human retina. *Invest. Ophthalmol. & Visual Sci.* 26:58-67.

33. Hollyfield, J. G., H. H. Varner, M. F. Rayborn, G. I. Liou, and C. D. B. Bridges. 1985. Endocytosis and degradation of interstitial retinol-binding protein: differential capabilities of cells that border the interphotoreceptor matrix. *J. Cell Biol.* 100:1676-1681.

34. Huynh, T. V., R. A. Yound, and R. W. Davis. 1985. Constructing and screening cDNA libraries in λgt 10 and λt 11. *In* DNA Cloning, a Practical Approach. D. M. Glover, editor. IRL Press, Oxford, England. 49-78.

35. Inouye, L. N., A. Albini, G. J. Chader, T. M. Redmond, and J. M. Nickerson. 1989. mRNA for interphotoreceptor retinoid-binding protein (IRBP): distribution and size diversity in vertebrate species. *Exp. Eye Res.* 49:171-180.

36. Johnson, A. T., F. L. Kretzer, H. M. Hittner, P. A. Glazebrook, C. D. B. Bridges, and D. M. K. Lam. 1985. Development of the subretinal space in the preterm human eye: ultrastructural and immunocytochemical studies. *J. Comp. Neurol.* 233:497-505.

37. Jones, G. J., R. K. Crouch, B. Wiggert, M. C. Cornwall, and G. J. Chader. 1989. Retinoid requirements for recovery of sensitivity after visual-pigment bleaching in isolated photoreceptors. *Proc. Natl. Acad. Sci. USA.* 86:9606-9610.

38. Lai, Y. L., B. Wiggert, Y. P. Liu, and G. J. Chader. 1982. Interphotoreceptor retinoid-binding proteins: possible transport vehicles between compartments of the retina. *Nature (Lond.).* 298:848-849.

39. LaVail, M. M., L. H. Pinto, and D. Yasumura. 1981. The interphotoreceptor matrix in rats with inherited retinal dystrophy. *Invest. Ophthalmol. & Visual Sci.* 21:658-668.

40. Lee, J. J., and N. A. Costlow. 1987. A molecular titration assay to measure transcript prevalence levels. *Methods Enzymol* 152:633-648.

41. Lin, Zhen-Shi, S.-L. Fong, and C. D. B. Bridges. 1989. Retinoids bound to interstitial retinol-binding protein during light and dark-adaptation. *Vision Res.* 29:1699-1709.

42. Liou, G. I., C. D. B. Bridges, S.-L. Fong, R. A. Alvarez, and F. Gonzalez-Fernandez. 1982. Vitamin A transport between retina and pigment epithelium—an interstitial protein carrying endogenous retinal (interstitial retinol-binding protein). *Vision Res.* 22:1457-1467.

43. Liou, G. I., S.-L. Fong, W. G. Beattie, R. G. Cook, J. Leone, R. A. Landers, R. A. Alvarez, C. Wang, Y. Li, and C. D. B. Bridges. 1986. Bovine interstitial retinol-binding protein (IRBP)-isolation and sequence analysis of cDNa clones, characterization and *in vitro* translation of mRNA. *Vision Res.* 26:1645-1653.

44. Liou, G. I., S.-L. Fong, J. Gosden, P. V. Tuinen, D. H. Ledbetter, S. Christie, D. Rout, S. Bhattacharya, R. G. Cook, L. Li, C. Wang, and C. D. B. Bridges. 1987. Human interstitial retinol-binding protein (IRBP): cloning, partial sequence, and chromosomal localization. *Somatic Cell Mol. Genet.* 13:315-323.

45. Liou, G. J., D.-P. Ma, Y.-W. Yeng, L. Geng, C. Zhu, and W. Baehr. 1989. Human interstitial-retinol binding protein: gene structure and primary sequence. *J. Biol. Chem.* 264:8200-8206.

46. Maniatis, T., E. F. Fritsch, and J. Sambrook. 1982. Molecular Cloning: A Laboratory Manual. Cold Spring Harbor Laboratory, Cold Spring Harbor, New York. 545 pp.

47. Okajima, T.-I. L., D. R. Pepperberg, H. Ripps, B. Wiggert, and G. J. Chader. 1989. Interphotoreceptor retinoid-binding protein: role in delivery of retinol to the pigment epithelium. *Exp. Eye Res.* 49:629-644.

48. Perez-Castro, A. V., L. E. Toth-Rogler, L.-N. Wei, and M. C. Nguyen-huu. 1989. Spatial and temporal pattern of expression of the cellular retinoic acid-binding protein and the cellular retinol-binding protein during mouse embryogenesis. *Proc. Natl. Acad. Sci. USA.* 86:8813-8817.

49. Pfeffer, B., B. Wiggert, L. Lee, B. Zonnenberg, and G. J. Chader. 1983. The presence of a soluble interphotoreceptor retinol-binding protein (IRBP) in the retinal interphotoreceptor space. *J. Cell. Physiol.* 117:333.

50. Politi, L. E., L. Lee, B. Wiggert, G. Chader, and R. Adler. 1989. Synthesis and secretion of interphotoreceptor retinoid-binding protein (IRBP) by isolated normal and rd mouse retinal photoreceptor neurons in culture. *J. Cell. Phys.* 141:682-690.

51. Saari, J. C., D. C. Teller, J. W. Crabb, and L. Bredberg. 1985. Properties of an interphotoreceptor retinoid-binding protein from bovine retina. *J. Biol. Chem.* 260:195-201.

52. Schneider, B. B., D. S. Papermaster, G. I. Liou, S.-L. Fong, and C. D. B. Bridges. 1986. Electron microscopic immunocytochemistry of interstitial retinol-binding protein in vertebrate retinas. *Invest. Opthalmol. & Visual Sci.* 27:679-688.

53. Si, J.-S., D. E. Brost, T. M. Redmond, and J. M. Nickerson. 1989. Cloning of cDNAs encoding human interphotoreceptor retinoid-binding protein (IRBP) and comparison with bovine IRBP sequences. *Gene.* 80:99-108.

54. Taniguchi, T., A. J. Adler, T. Mizuochi, N. Kochibe, and A. Kobata. 1986. The structures of the asparagine-linked sugar chains of bovine interphotoreceptor retinol-binding protein. *J. Biol. Chem.* 261:1730-1736.

55. Treisman, J. E., M. A. Morabito, and C. J. Barnstable. 1988. Opsin expression in the rat retina is developmentally regulated by transcriptional activation. *Mol. Cell. Biol.* 8:1570-1579.

56. Veen, T. van, A. Katial, T. Shinohara, D. J. Barrett, B. Wiggert, G. J. Chader, and J. M. Nickerson. 1986. Retinal photoreceptor neurons and pinealocytes accumulate mRNA for interphotoreceptor retinoid-binding protein (IRBP). *FEBS (Fed. Eur. Biochem. Soc.) Lett.* 208:133-137.

57. Vehara, F., M. T. Matthes, D. Yasumura, and M. M. Lavail. 1990. Light-evoked changes in the interphotoreceptor matrix. *Science (Wash. DC).* 248:1633-1636.

58. Vollmer, G., and P. G. Layer. 1986. An *in vitro* model of proliferation and differentiation of chick retina: coaggregates of retinal and pigment epithelial cells. *J. Neurosci.* 6:1885-1896.

59. Weidman, T. A., and T. Kuwabara. 1968. Postnatal development of the rat retina: an electron microscopic study. *Arch. Ophthalmol.* 79:470-484.

60. Zauberman, H. 1979. Adhesive forces between the retinal pigment epithelium and sensory retina. *In*: The Retinal Pigment Epithelium. K. M. Zinn and M. F. Marmor, editors. Harvard University Press, Cambridge, MA. 192-204.

61. Zimmerman, L. E., and A. B. Eastham. 1959. Acid mucopolysaccharide in the retinal pigment epithelium and visual cell layer of the developing mouse eye. *Am. J. Ophthal.* 47:488-498.